Chemistry and Materials

The Center for Science Innovation

Research Article

Chem. Mater. 3 (1) 2024, 21-26

Square-Wave Pulse Deposition of Pt Nanoparticles for Ethanol Electrooxidation

Hilman Syafei[1], Devi Indrawati Syafei[2,*]

[1]The Center for Science Innovation, Jakarta Timur 13120, Indonesia

[2]National Taiwan University No.1, Section 4, Roosevelt Rd, Da'an District, Taipei City, Taiwan

*Corresponding author: r11527984@ntu.edu.tw

Received
31 December 2024

Received in revised form
12 February 2024

Accepted
23 February 2024

Published online
29 February 2024

DOI
https://doi.org/10.56425/cma.v3i1.70

Abstract

Platinum (Pt) is often used as an electrocatalyst in the electrooxidation of ethanol. There have been many attempts to improve the catalytic properties of platinum-based catalysts to achieve satisfactory results. The solutions are manipulating the size and shape of Pt. In this study, Pt will be deposited using the square wave pulse deposition method at upper potential variations. The Pt samples were characterized by scanning electron microscopy (SEM), X-ray diffraction, energy dispersive X-ray, and electrochemical impedance spectroscopy. The results of SEM show that the morphology of Pt at potentials of 0.3 V, 0.5 V, and 1.0 V produces a dendritic nanothorn morphology, while 1.25 V and 1.50 V produce a nanoleaf morphology. The lowest charge transfer resistance value is at $Pt_{1.0V}$ with the smallest size. The highest yield of ethanol electrooxidation was at $Pt_{1.0V}$ reaching 8.82 mA/cm^2.

Keywords: electrocatalyst, platinum, ethanol electrooxidation.

1. Introduction

Air pollution and global warming due to fossil fuels are a concern for the whole world crisis environmental crisis. The solution is to utilize renewable resources whose gas emissions are not harmful to the environment. Direct ethanol fuel cell is one of the solutions offered to replace fossil fuels [1]. The advantages offered are that the energy density produced is quite large, environmentally safer, easy to store, has low toxicity, and can be carried out at room temperature [2,3].

The problem in the process of obtaining electrical energy from ethanol electrooxidation lies in the catalyst. Catalyst development is needed for the process of breaking down the C-C bond in ethanol into CO_2 gas [4]. Platinum (Pt) is one of the catalysts of interest for the ethanol electrooxidation process. This is because Pt has high catalytic activity and can work at room temperature for the ethanol electrooxidation process [5].

Studies have found that Pt is effective as an electrocatalyst in ethanol electrooxidation [6–10]. The effectiveness of the Pt-catalyst can be further increased by reducing the particle size to nanosize [11,12] and the morphology of the catalyst can be manipulated to increase the contact area of ethanol electrooxidation [13,14]. Manipulating the size and shape of the Pt-catalyst seems promising to increase ethanol electrooxidation activity. One of the synthesis methods of nanoparticles that is easy to manipulate in terms of size and shape of the Pt-catalyst is square wave pulse deposition.

The Pt-based catalyst will be synthesized using the square wave pulse deposition method to obtain the expected size and morphology [6]. Manipulation of size and morphology can be obtained using several factors, one of which is the applied potential in stimulator mode [6,15]. To synthesize Pt-based catalysts with a variety of sizes and morphologies, the upper potential will be varied during the research process.

2. Materials and Method

The method used for the synthesis of this Pt-based catalyst is square wave pulse deposition at room temperature. The solution used is K_2PtCl_6 at 1 mM and dissolved in a 1.0 M H_2SO_4 electrolyte solution. Other chemicals used in the research are KCl, NaOH, and ethanol 96% with Merck analytical chemical specifications. Electrodeposition was carried out using a three-electrode

system (eDAQ ER 466 potentiostat). The working electrode used is fluorine-doped tin oxide (FTO) 0.5x0.3 cm, the counter electrode is Pt wire, and the reference electrode is Ag/AgCl (KCl 3 M). The FTO was then washed with aquadest and ethanol (p.a) and then dried briefly. Electrodeposition will be carried out using a lower potential at -0.3 V and varying upper potentials at 0.3, 0.5, 1.0, 1.25, and 1.50 V for 10 minutes. The results of the Pt synthesis are then rinsed and dried for the characterization process using X-ray diffraction Cu Kα (XRD, PANalytical AERIS) to determine the Pt phase (with 2θ 20° – 70°), field emission scanning electron microscopy (FESEM, Thermo Scientific Quattro S) to observe the morphology formed, energy dispersive x-ray (EDX, EDAX Apollo X) to determine the formation of the Pt formed, electrochemical impedance spectroscopy (EIS) with electrochemical workstation (Corrtest CS310) at a frequency of 50 kHz to 0.1 kHz with a 0.5 M KCl solution. The ethanol electrooxidation test was then carried out using a solution of 1.0 M ethanol and 0.1 M NaOH.

3. Results and Discussion

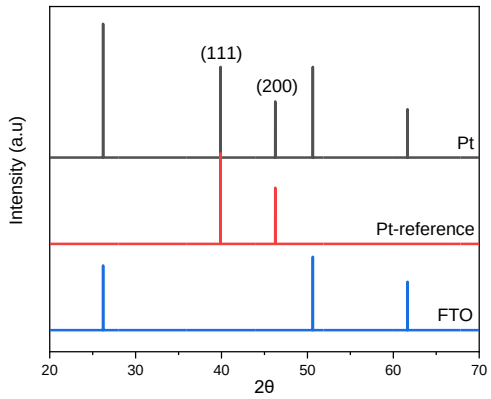

Figure 1. XRD pattern of Pt

The XRD pattern of platinum synthesized with upper potential is shown in Fig. 1. The XRD pattern recorded platinum peaks at 39.89° and 46.25°, corresponding to the planes (111) and (200), respectively, which were consistent with face-centered cubic [16–18]. Other peaks that were originally recorded come from the FTO substrate [19] because of the thinness of the Pt layer.

Figure 2 shows the morphology of platinum synthesized at a lower potential (E_L) of -0.3 V with variations in the upper potential (E_U) of 0.3 V, 0.5 V, 1.0 V, 1.25 V, and 1.50 V. The applied potential will affect nucleation and growth. The initial nucleation of Pt starts with the reduction of Pt ions. The study by Malek et al. (2019) and Zhang et al. (2010) states that the effective potential for Pt nucleation is -0.2 V; if more positive potential is applied, Pt will slowly nucleate [20,21], followed by Pt growth at nucleated Pt sites with a sharp tip. Pt particles will likely grow in the sharp tips of the morphologies because of the difference in concentration between different areas. Therefore, Pt growth is more directed towards the tip site at the beginning of Pt nucleation because more concentrated Pt at the tip site [22]. The results of this growth form a dendritic nanothorn morphology, which can be observed in Fig. 2.

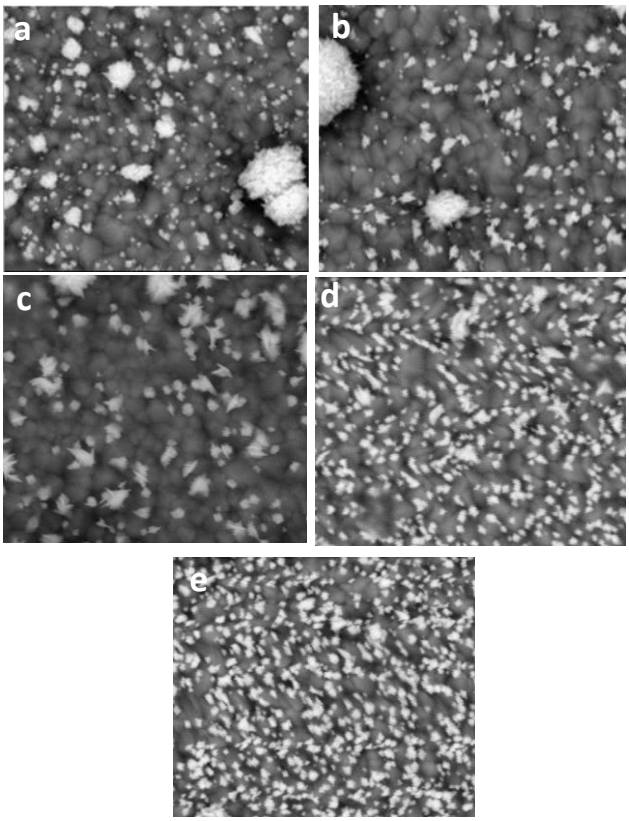

Figure 2. Platinum-catalyst morphologies with upper potential (a) 0.3 V, (b) 0.5 V, (c) 1.0 V, (d) 1.25 V, (e) 1.50 V.

The electrodeposition process using different potentials produces different morphologies and sizes. In E_U samples at 0.3 V and 0.5 V, the Pt particles experienced agglomeration and the morphology shown was non-uniform nanothorns. Agglomeration is caused by adhesion between particles, where the growth of particles on top of other particles (overlapping) occurs due to the force on a particle that can attract other particles [23]. In addition, Pt synthesized with E_U above 1.0 V can be oxidized to the oxide compound and form PtO_2. The study states that Pt can be oxidized at a potential of 1.25 V and can form other larger compounds, like $PtO_2.nH_2O$. The more positive the potential applied, the larger the particle size will be formed [24]. Therefore, the dendritic nano thorns on Pt with E_U above 1.0 V form a nano leaf-like morphology. The study

by Tian et al. (2006) states that lower potentials above -0.1 V will make nano thorns difficult to observe, while upper potentials exceeding 1.0 V will make the spines on nano thorns become blunt and form nanoleaf [25]. The particle size of each E_U variation Pt sample can be seen in Figure 2. The E_U variation Pt size is 63.0 nm for $Pt_{0.3V}$, 68.0 nm for $Pt_{0.5V}$, and 61.0 nm for $P_{1.0V}$. On the other hand, particle sizes for $Pt_{1.25V}$ and $Pt_{1.50V}$ with nanoleaf morphology are 69.0 nm and 76.0 nm, respectively. Therefore, the best distribution and morphology are found in EU 1.0 V synthesis conditions.

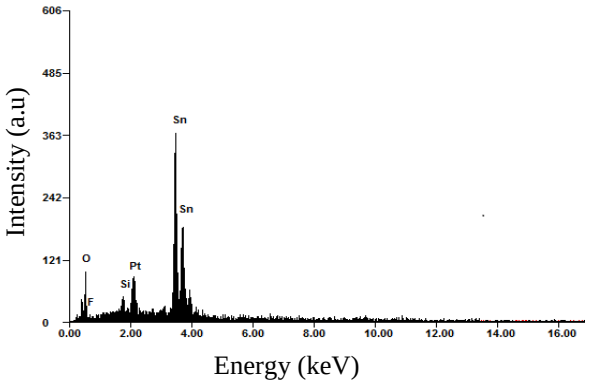

Figure 3. EDX spectrum of Pt nanocatalyst deposited in E_u 1.0 V and E_L -0.3 V.

Figure 3 shows the EDX spectrum results of the Pt catalyst synthesized on the FTO substrate. The peak signal that appears at 2.0 – 2.5 keV is Pt. The study by Naderi et al. (2012) stated that Pt was detected at signals between 2.0 and 2.5 keV [26]. Other elements such as Sn, Si, and F were detected in the FTO-glass substrate.

Figure 4 is a Nyquist plot of Pt with an upper potential of 0.3 V, 0.5V, 1.0V, 1.25V, and 1.50 V at a lower potential of -0.3 V. Based on these data, the smallest R_{ct} is obtained at an upper potential of $Pt_{1.0V}$. In the Nyquist plot, the R_s value, or solution resistance, in different samples has different values. This difference is due to the different morphology of Pt under E_U variations, so the initial response to solution resistance will be different [27]. The morphology of the sample in Figure 2 shows that Pt with an upper potential of 1.0 V has nano thorn dendritic morphology, but Pt synthesized above 1.0 V has nano leaf morphology that has a different surface area. The Nanoleaf morphologies in Figure 2 show a buildup of morphology that causes the surface area to not be as large as that of the dendritic nanothorn, so the initial response can affect the R_s value. Apart from that, the factor of small particle size and particle distribution influences the resistance of the samples [28,29]. A smaller particle size has affected ionic movement in the test because the distance it travels will be smaller, which will increase the movement of the ions. The smaller the R_{ct} value, the greater the electrical conductivity, which causes the electron transfer kinetics and catalytic process to happen faster [30].

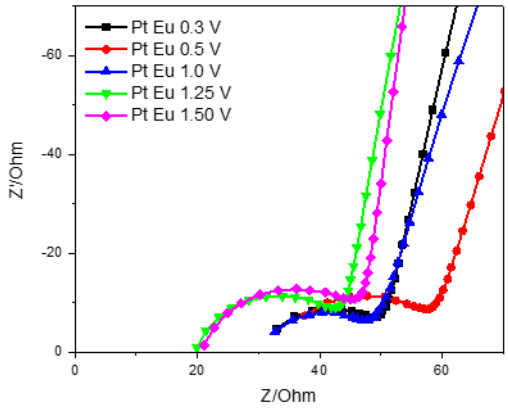

Figure 4. Nyquist plot of Pt electrocatalyst with various applied upper potential

Figure 5 is a voltammogram of ethanol electrooxidation using a platinum-catalyst with variations in upper potential. Differences in upper potential produce different peaks of electric current. The results of ethanol electrooxidation are presented in Table 1.

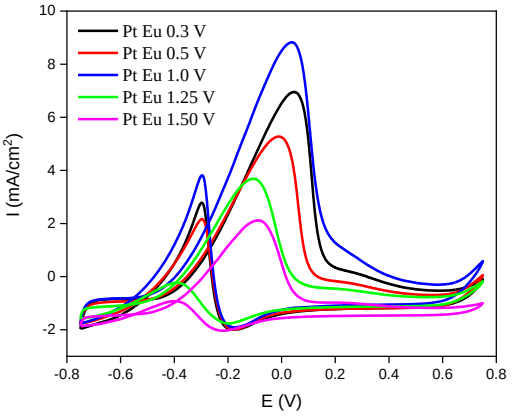

Figure 5. Ethanol electrooxidation of Pt electrocatalyst.

Table 1. Interpretation of ethanol electrooxidation in Pt with various applied upper potential

Sample	I_f (mA/cm^2)	I_b (mA/cm^2)	I_f/I_b	EASA (cm^{-2})
Pt Eu 0.3 V	6.94	2.78	2.50	47,51

Sample	I_f (mA/cm^2)	I_b (mA/cm^2)	I_f/I_b	EASA (cm^{-2})
Pt Eu 0.5 V	5.28	2.17	2.43	33,49
Pt Eu 1.0 V	8.82	3.80	2.32	59,34
Pt Eu 1.25 V	3.69	-0.26	-14.19	20,51
Pt Eu 1.50 V	2.13	-0.93	-2.29	11,94

Upper potential variation consisting of Pt with E_U 0.3 V, 0.5 V, 1.0 V, 1.25 V, and 1.50 V at E_L -0.3 V produces an electric current of, respectively, 6.94 mA/cm^2, 5.28 mA/ cm^2, 8.82 mA/ cm^2, 3.69 mA/ cm^2, and 2.13 mA/ cm^2. In Figure 5, the difference in upper potential gives variations in the yield of oxidized ethanol in the form of electric current density during the process of oxidizing ethanol to CO_2. The higher the electric current value, the more ethanol is oxidized to CO_2 because complete oxidation of ethanol will produce 12 e-. The mechanism that occurs during ethanol electrooxidation is as follows: [31]

C1 pathway:

$$C_2H_5OH \longrightarrow CO_X + CH_X \longrightarrow CO_2 + 12e^- \quad (1)$$

C2 pathway:

$$C_2H_5OH \longrightarrow CH_3CHO \longrightarrow CH_3COOH + 4e^- \quad (2)$$

Two pathways of ethanol electrooxidation can occur during the ethanol electrooxidation process (the C1/C2 pathway). This second pathway has different results at the end of the process, where the C1 pathway will produce CO_{ads} or CO_2 and 12 e^-, while the C2 pathway will produce acetic acid (CH_3COOH) and 4 e^- [31]. Ethanol (C_2H_5OH), which is adsorbed on the electrode surface, can then be split or undergo C-C bond breaking to form an acetic acid phase, which requires low energy, or forms CO_2, which requires large energy [32]. A study from Ferre-Vilaplana states that the breaking of the C-C bond in ethanol begins to appear at a potential of 0.2 V and CO_2 begins to form at a potential below 0.5 V [33]. The difference in potential or the occurrence of a potential shift that is different from the reference indicates the presence of a different platinum lattice. It causes better dissociation to produce OH_{ads} [34].

The highest ethanol electrooxidation was $Pt_{1.0V}$, with a value of 8.82 mA/cm^2. This matches the best size and morphology of $Pt_{1.0V}$ compared to Pt with other upper-potential variations. This data is matched by the electrochemical surface area (EASA) value shown in Table 1. A large EASA value indicates that the active surface of the catalyst for the electrooxidation process will be higher. The formula of EASA used is:

$$EASA = \frac{Q_{CO} x\ A}{Q_{Pt}} \quad (3)$$

Which, Q_{CO} is the charge calculated during the EOR process, Q_{Pt} is the charge released on the surface (210 µC/cm^2), and A is the surface area of the catalyst [35].

The stability of the electrocatalyst can be seen from the comparison value between I_f/I_b in Table 1. A large I_f/I_b value indicates that the stability of the electrocatalyst is higher than others [36]. In Table 1, $Pt_{1.0V}$ has the largest I_f/I_b value, which indicates that $Pt_{1.0V}$ has the best poisoning tolerance. Therefore, $Pt_{1.0V}$ is Pt with optimum results with a more dispersed dendritic nanothorn morphology, a low R_{ct} value, and the best ethanol electrooxidation activity.

4. Conclusion

Pt-based catalysts have been successfully synthesized using variations in voltage. Variations in the upper voltage result in morphological changes at an upper voltage above 1.0 V compared to a voltage of 1.0 V. This can occur because the Pt nanothorn growth process effectively occurs at an upper voltage of 1.0 V. The results of the EIS characterization also show that $Pt_{1.0V}$ produces the lowest R_{ct} value due to its size, which produces smaller and more dispersed Pt particles. The best ethanol electrooxidation test was obtained on a $Pt_{1.0V}$ catalyst with a value of 8.82 mA/cm^2. This result is supported by the best nanothorn size and morphology on the $Pt_{1.0V}$ catalyst and the lowest R_{ct} value on the $Pt_{1.0V}$ catalyst.

Acknowledgment

Acknowledge funder or institution that supported the reported research.

References

[1] H. Burhan, M. Yılmaz, K. Cellat, A. Zeytun, G. Yılmaz, F. Şen, Direct ethanol fuel cells (DEFCs), in: Direct Liq. Fuel Cells, Elsevier, 2021: pp. 95–113. https://doi.org/10.1016/b978-0-12-818624-4.00004-2.

[2] J. Liu, Y. Zheng, S. Hou, Facile synthesis of Cu/Ni alloy nanospheres with tunable size and elemental ratio, *RSC Adv.* **7** (2017) 37823–37829. https://doi.org/10.1039/c7ra06062a.

[3] S. Mostrou, A. Nagl, M. Ranocchiari, K. Föttinger, J.A. Van Bokhoven, The catalytic and radical mechanism for ethanol oxidation to acetic acid, *Chem. Commun.* **55** (2019) 11833–11836. https://doi.org/10.1039/c9cc05813c.

[4] M. Veligatla, S. Katakam, S. Das, N. Dahotre, R.

Gopalan, D. Prabhu, D. Arvindha Babu, H. Choi-Yim, S. Mukherjee, Effect of Iron on the Enhancement of Magnetic Properties for Cobalt-Based Soft Magnetic Metallic Glasses, *Metall. Mater. Trans. A*. **46** (2015) 1019–1023. https://doi.org/10.1007/s11661-014-2714-2.

[5] A. Li, W. Duan, J. Liu, K. Zhuo, Y. Chen, J. Wang, Electrochemical synthesis of AuPt nanoflowers in deep eutectic solvent at low temperature and their application in organic electro-oxidation, *Sci. Rep.* **8** (2018). https://doi.org/10.1038/s41598-018-314029.

[6] A. Sabella, Reyhan Syifa, N.A. Dwiyana, The Effect of Deposition Potential on the Electrodeposition of Platinum Nanoparticles for Ethanol Electrooxidation, *Chem. Mater.* **1** (2022) 88–92. https://doi.org/10.56425/cma.v1i3.46.

[7] J. Ma, H. Sun, F. Su, Y. Chen, Y. Tang, T. Lu, J. Zheng, Ethanol electrooxidation on carbon-supported Pt nanoparticles catalyst prepared using complexing self-reduction method, *Int. J. Hydrogen Energy*. **36** (2011) 7265–7274. https://doi.org/10.1016/j.ijhydene.2011.02.142.

[8] A. Ghumman, C. Vink, O. Yepez, P.G. Pickup, Continuous monitoring of CO2 yields from electrochemical oxidation of ethanol: Catalyst, current density and temperature effects, *J. Power Sources*. **177** (2008) 71–76. https://doi.org/10.1016/j.jpowsour.2007.11.009.

[9] D.J. Guo, X.P. Qiu, L.Q. Chen, W.T. Zhu, Multi-walled carbon nanotubes modified by sulfated TiO2 - A promising support for Pt catalyst in a direct ethanol fuel cell, *Carbon N. Y.* **47** (2009) 1680–1685. https://doi.org/10.1016/j.carbon.2009.02.023.

[10] W.P. Zhou, M. Li, C. Koenigsmann, C. Ma, S.S. Wong, R.R. Adzic, Morphology-dependent activity of Pt nanocatalysts for ethanol oxidation in acidic media: Nanowires versus nanoparticles, *Electrochim. Acta*. **56** (2011) 9824–9830. https://doi.org/10.1016/j.electacta.2011.08.055.

[11] Y. Tang, S. Cao, Y. Chen, T. Lu, Y. Zhou, L. Lu, J. Bao, Effect of Fe state on electrocatalytic activity of Pd-Fe/C catalyst for oxygen reduction, *Appl. Surf. Sci.* **256** (2010) 4196–4200 . https://doi.org/10.1016/j.apsusc.2010.01.124.

[12] A. Chen, P. Holt-hindle, Platinum-Based Nanostructured Materials : Synthesis , Properties , and Applications, (2010) 3767–3804.

[13] C. Li, H. Wen, P.P. Tang, X.P. Wen, L.S. Wu, H. Bin Dai, P. Wang, Effects of Ni(OH)2 Morphology on the Catalytic Performance of Pd/Ni(OH)2/Ni Foam Hybrid Catalyst toward Ethanol Electrooxidation, *ACS Appl. Energy Mater.* **1** (2018) 6040–6046 . https://doi.org/10.1021/acsaem.8b01095.

[14] R.C. Cerritos, M. Guerra-Balcázar, R.F. Ramírez, J. Ledesma-García, L.G. Arriaga, Morphological effect of Pd catalyst on ethanol electro-oxidation reaction, *Materials (Basel).* **5** (2012) 1686–1697. https://doi.org/10.3390/ma5091686.

[15] S. Gautam, A.M.K. Hadley, B.D. Gates, Controlled Growth of Platinum Nanoparticles during Electrodeposition using Halide Ion Containing Additives, *J. Electrochem. Soc.* **169** (2022) 112508. https://doi.org/10.1149/1945-7111/ac9e22.

[16] M.N. Kumar, B. Govindh, N. Annapurna, Green synthesis and characterization of platinum nanoparticles using Sapindus mukorossi Gaertn. fruit pericarp, *Asian J. Chem.* **29** (2017) 2541–2544. https://doi.org/10.14233/ajchem.2017.20842A.

[17] M. Gholami-Shabani, M. Shams-Ghahfarokhi, Z. Gholami-Shabani, A. Akbarzadeh, G. Riazi, M. Razzaghi-Abyaneh, Biogenic Approach using Sheep Milk for the Synthesis of Platinum Nanoparticles: The Role of Milk Protein in Platinum Reduction and Stabilization, 2016. https://www.researchgate.net/publication/311086217.

[18] T.L. Nguyen, V.H. Cao, T. Hai, Y. Pham, T.G. Le, Platinum Nanoflower-Modified Electrode as a Sensitive Sensor for Simultaneous Detection of Lead and Cadmium at Trace Levels, **2019** (2019).

[19] S.A. Lee, I.J. Park, J.W. Yang, J. Park, T.H. Lee, C. Kim, J. Moon, J.Y. Kim, H.W. Jang, Electrodeposited Heterogeneous Nickel-Based Catalysts on Silicon for Efficient Sunlight-Assisted Water Splitting, *Cell Reports Phys. Sci.* **1** (2020) 100219. https://doi.org/10.1016/j.xcrp.2020.100219.

[20] N.S.A. Malek, Y. Mohd, EFFECT OF DEPOSITION TIME ON STRUCTURAL AND CATALYTIC PROPERTIES OF Pt FILMS ELECTRODEPOSITED ON Ti SUBSTRATE, *Malaysian J. Anal. Sci.* **23** (2019) 52–59.

[21] H. Zhang, W. Zhou, Y. Du, P. Yang, C. Wang, One-step electrodeposition of platinum nanoflowers and their high efficient catalytic activity for methanol electro-oxidation, *Electrochem. Commun.* **12** (2010) 882–885. https://doi.org/10.1016/j.elecom.2010.04.011.

[22] V. Palmre, D. Pugal, K.J. Kim, K.K. Leang, K. Asaka, A. Aabloo, Nanothorn electrodes for ionic polymer-metal composite artificial muscles, *Sci. Rep.* **4** (2014). https://doi.org/10.1038/srep06176.

[23] M.A. Ashraf, W. Peng, Y. Zare, K.Y. Rhee, Effects of Size and Aggregation/Agglomeration of Nanoparticles on the Interfacial/Interphase Properties and Tensile Strength of Polymer Nanocomposites, *Nanoscale Res. Lett.* **13** (2018). https://doi.org/10.1186/s11671-018-2624-0.

[24] R. Mom, L. Frevel, J.J. Velasco-Vélez, M. Plodinec, A. Knop-Gericke, R. Schlögl, The Oxidation of Platinum

under Wet Conditions Observed by Electrochemical X-ray Photoelectron Spectroscopy, *J. Am. Chem. Soc.* **141** (2019) 6537–6544. https://doi.org/10.1021/jacs.8b12284.

[25] N. Tian, Z.Y. Zhou, S.G. Sun, L. Cui, B. Ren, Z.Q. Tian, Electrochemical preparation of platinum nanothorn assemblies with high surface enhanced Raman scattering activity, *Chem. Commun.* (2006) 4090–4092. https://doi.org/10.1039/b609164d.

[26] N. Naderi, M.R. Hashim, J. Rouhi, N. Naderi, J. Rouhi, Synthesis and Characterization of Pt Nanowires Electrodeposited into the Cylindrical Pores of Polycarbonate Membranes, 2012. www.electrochemsci.org.

[27] A. Abdelgawad, B. Salah, K. Eid, A.M. Abdullah, R.S. Al-Hajri, M. Al-Abri, M.K. Hassan, L.A. Al-Sulaiti, D. Ahmadaliev, K.I. Ozoemena, Pt-Based Nanostructures for Electrochemical Oxidation of CO: Unveiling the Effect of Shapes and Electrolytes, *Int. J. Mol. Sci.* **23** (2022). https://doi.org/10.3390/ijms232315034.

[28] P. Ghosh, R.N. Bhowmik, S. Bandyopadhyay, P. Mitra, Influence of Particle Size on the Electrical Properties and Magnetic Field Dependent I–V Characteristics of Nanocrystalline ZnFe2O4, *Trans. Indian Ceram. Soc.* **78** (2019) 111–120. https://doi.org/10.1080/0371750X.2019.162461.

[29] M. Hennemann, M. Gastl, T. Becker, Influence of particle size uniformity on the filter cake resistance of physically and chemically modified fine particles, *Sep. Purif. Technol.* **272** (2021). https://doi.org/10.1016/j.seppur.2021.118966.

[30] H. Syafei, Dwi Giwang Kurniawan, Electrodeposition of CoxNiy Thin Film and Its Catalytic Activity for Ethanol Electrooxidation, *Chem. Mater.* **2** (2023) 14–18. https://doi.org/10.56425/cma.v2i1.50.

[31] J. Flórez-Montaño, G. García, O. Guillén-Villafuerte, J.L. Rodríguez, G.A. Planes, E. Pastor, Mechanism of ethanol electrooxidation on mesoporous Pt electrode in acidic medium studied by a novel electrochemical mass spectrometry set-up, *Electrochim. Acta*. **209** (2016) 121–131. https://doi.org/10.1016/j.electacta.2016.05.070.

[32] T. Sheng, C. Qiu, X. Lin, W.F. Lin, S.G. Sun, Insights into ethanol electro-oxidation over solvated Pt(1 0 0): Origin of selectivity and kinetics revealed by DFT, *Appl. Surf. Sci.* **533** (2020). https://doi.org/10.1016/j.apsusc.2020.147505.

[33] A. Ferre-Vilaplana, C. Buso-Rogero, J.M. Feliu, E. Herrero, Cleavage of the C-C Bond in the Ethanol Oxidation Reaction on Platinum. Insight from Experiments and Calculations, *J. Phys. Chem. C*. **120** (2016) 11590–11597. https://doi.org/10.1021/acs.jpcc.6b03117.

[34] Y. Wang, S. Zou, W. Bin Cai, Recent advances on electro-oxidation of ethanol on Pt- and Pd-based catalysts: From reaction mechanisms to catalytic materials, *Catalysts*. **5** (2015) 1507–1534. https://doi.org/10.3390/catal5031507.

[35] F.P. Lohmann-Richters, B. Abel, Á. Varga, In situ determination of the electrochemically active platinum surface area: Key to improvement of solid acid fuel cells, *J. Mater. Chem. A*. **6** (2018) 2700–2707. https://doi.org/10.1039/c7ta10110d.

[36] S.S. Gwebu, N.W. Maxakato, The influence of ZrO2 promoter in Pd/fCNDs-ZrO2 catalyst towards alcohol fuel electrooxidation in alkaline media, *Mater. Res. Express*. **7** (2019). https://doi.org/10.1088/2053-1591/ab640e.